Rate of human motor adaptation under varying system dynamics

Conference Paper · June 2011

DOI: 10.1109/WHC.2011.5945480 · Source: DBLP

4 authors:

Ahmetcan Erdogan
Rehabilitation Institute of Chicago

Ali Israr
Facebook

Marcia Kilchenman O'Malley
Rice University

Volkan Patoglu
Sabanci University

Rate of Human Motor Adaptation under Varying System Dynamics

Ahmetcan Erdogan*
Sabancı University
İstanbul, TURKEY

Ali Israr†
Rice University
Houston, TX, USA

Marcia K. O'Malley‡
Rice University
Houston, TX, USA

Volkan Patoglu§
Sabancı University
İstanbul, TURKEY

Abstract

We explore the effects of parameters constituting a second order dynamic system on the rate of human motor adaptation while performing a rhythmic dynamic task. In our experiments, participants excite virtual second-order systems at resonance via a haptic interface. After overtraining subjects with a nominal system, we unexpectedly change the system parameters and study the resulting motor adaptation in catch trials. Through four experiment seatings, we demonstrate the effects of dynamic system parameters on human motor adaptation. Results indicate that gain and damping parameters significantly affect the rate of adaptation. In particular, as the effort required to complete the task increases, the rate of adaptation decreases, indicating a trade-off between task performance and the effort required to perform the task.

1 Introduction

The human motor system is very adaptable and robust when it comes to experiencing new dynamic environments. In particular, when the dynamics of a task are altered, the sensorimotor system detects these changes and fine tunes control parameters of a pre-existing internal model in order to compensate for the varying dynamics of the task [11]. In the literature, it has been shown that humans can adapt their feed-forward control commands over time [10, 2] and this adaptation can be viewed as successful training of a new skill. Psychophysical analysis of human interactions with new dynamic systems may shed light on the mechanisms used by humans to execute motor tasks. A broader understanding of human motor control could directly benefit researchers who develop training protocols or simulations to teach new motor skills.

The relevant literature has focused on learning and adaptation of humans while performing point-to-point reaching movements under normal and augmented environmental conditions [1, 8], while the influence of dynamic parameters on human motor behavior while performing *dynamic tasks* has received much less attention [13, 3]. Dynamic tasks, such as pumping a swing or bouncing a ball, are different from simple reaching movements in that the dynamic behavior of the environment directly affects the control input planned and executed by the user [12].

Huang *et al.* [4] investigated a simple rhythmic dynamic object manipulation task in a virtual environment and determined that participants could identify and excite distinct virtual system natural frequencies with visual only, haptic only, or combined visual and haptic feedback. They observed that participants tuned their control parameters as a general feedback strategy. Similarly, in our earlier study [6], we explored the effects of magnitude and phase cues on human motor adaptation and showed the persistent ability of humans to perform system identification of the dynamic systems which they control, regardless of the cue that was conveyed. In related studies, we have showed that the performance of the manual control task was influenced by the participant's ability to perform system identification in order to excite the virtual dynamic system near its resonant frequency [9, 5] and determined the just-noticeable-difference (JND) for natural frequency of virtual second-order dynamic systems to be in 4%-9% range for 1 Hz and 2 Hz reference natural frequencies with visual-, haptic, and visual+haptic feedback [7].

The objective of this paper is to investigate effects of parameters of a second order dynamic system on the rate of human motor adaptation while performing a rhythmic dynamic task. A linear mass-spring-damper system is studied, where the dynamics governing this second order system depend on the natural frequency w_n, damping ζ and gain G parameters.

When a virtual mass-spring-damper system is excited with rhythmic sinusoidal input motion, the system output behavior is characterized by its position and impedance transfer functions. In particular, the position transfer function maps the input excitation to the output motion of the virtual mass displayed on the screen, while the impedance transfer function maps the input excitation to the forces rendered back to the user. A change in gain of the transfer functions scales the output motion and affects the magnitude of forces felt by the user, while a change in damping strongly affects the characteristic of the dynamic system especially in the neighborhood of its natural frequency.

To this end, we conducted an experiment to investigate the effects of dynamic parameters on human motor adaptation to a manually excited virtual second-order system. We employed a "catch trial" procedure, which first overtrains the participant while exciting the dynamics of the nominal system. Then, in later trials, some features of the system are changed within the trial in order to monitor the participants' ability to identify and control the new target system that has different dynamic characteristics when compared to the nominal system. The goal of each catch session is to evaluate the effect of particular parameter sets on adaptation of hand excitation frequency between nominal and target system, primarily focusing on rate of adaptation and steady state error.

It is hypothesized that increasing the gain will help subjects better perceive the system dynamics, but at a cost of larger power input required to complete the task. Increasing damping is expected to have a stabilizing effect on human motor control, while perception of the natural frequency is diminished, thereby slowing adaptation.

2 Experimental Methods

In order to examine the rate of human adaptation to parameter variations of dynamic systems, an experiment is designed with a dynamic virtual reality environment. Experiments are conducted using a haptic device, a two degrees-of-freedom (DoF) planar manipulator, where one of the translational axes is used in order to excite the second order virtual system. Details of the mechanical system, the equation of motion governing the virtual system dynamics and the experiment design are detailed in this section.

2.1 Experimental Setup and Virtual Environment

The experimental setup consisted of a workstation running RTX real-time operating system, a flat-screen monitor and a 2 DoF planar haptic device (Pantograph by Quanser Inc.) as shown in Fig-

*e-mail:ahmetcan@sabanciuniv.edu
†e-mail: israr@disneyresearch.com
‡e-mail:omalleym@rice.edu
§e-mail:vpatoglu@sabanciuniv.edu

IEEE World Haptics Conference 2011
21-24 June, Istanbul, Turkey
978-1-4577-0297-6/11/$26.00 ©2011 IEEE

ure 2.1. The visual cues were updated at a rate of 50 Hz on the screen while the haptic rate was set at 500 Hz. Participants wore noise cancelation headphones playing pink noise to mask possible auditory cues from the environment and the hardware.

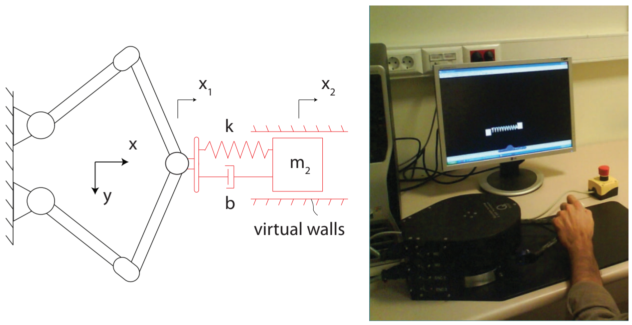

Figure 1: Experiment setup and the virtual environment

During the experiment, two rectangular masses were displayed on the screen. The motion of one mass, m_1, was directly coupled with the motion of the end-effector, while the second mass, m_2, was connected to m_1 by a virtual spring and damper resulting an indirect control over m_2. The instantaneous states (position, velocity and acceleration) of m_2 were calculated by the following second-order dynamic equation using Euler's method of numerical integration

$$m_2\,\ddot{x}_2 + b\,\dot{x}_2 + k\,x_2 = G\,(b\,\dot{x}_1 + k\,x_1) \qquad (1)$$

where $\dot{x}_1$ and x_1 are the velocity and displacement of m_1, respectively and $\ddot{x}_2$, $\dot{x}_2$ and x_2 are acceleration, velocity and displacement of m_2. G is the gain, b is the damping between two masses, while k represents the spring that attaches two masses together. The natural frequency and damping ratio of the second-order system can be calculated as $\omega_n = \sqrt{\frac{k}{m_2}}$ and $\zeta = \frac{b}{2\,\omega_n}$, respectively. The physical mass, damping and friction of the force feedback device are assumed to be negligible, since the pantograph mechanism is a high-fidelity impedance-type haptic interface. Hence, throughout the discussion, the human is assumed to be a perfect position source for the haptic device. The force F applied through the motors of the haptic device was calculated as

$$F = b\,(\dot{x}_2 - G\,\dot{x}_1) + k\,(x_2 - G\,x_1) \qquad (2)$$

The displacement transfer function between human position input and virtual mass position output is given as

$$\frac{X_2}{X_1} = \frac{G\,(2\,\zeta\,\omega_n\,s + \omega_n^2)}{s^2 + 2\,\zeta\,\omega_n\,s + \omega_n^2}. \qquad (3)$$

while the impedance transfer function between human position input and virtual force output is calculated as

$$\frac{F}{X_1} = \frac{G\,m_2\,s^2\,(2\,\zeta\,\omega_n\,s + \omega_n^2)}{s^2 + 2\,\zeta\,\omega_n\,s + \omega_n^2}. \qquad (4)$$

Note that the impedance transfer function is scaled by $m_2 s^2$ when compared with the position transfer function.

2.2 Participants

Seven healthy students of Sabancı University (six male, one female, 23–27 years old, average 24.7 years) participated in the study. All participants had prior experience with haptic devices. No participant reported any sensory or motor impairment. All participants signed informed consent forms approved by the University Research Ethics Council of Sabancı University.

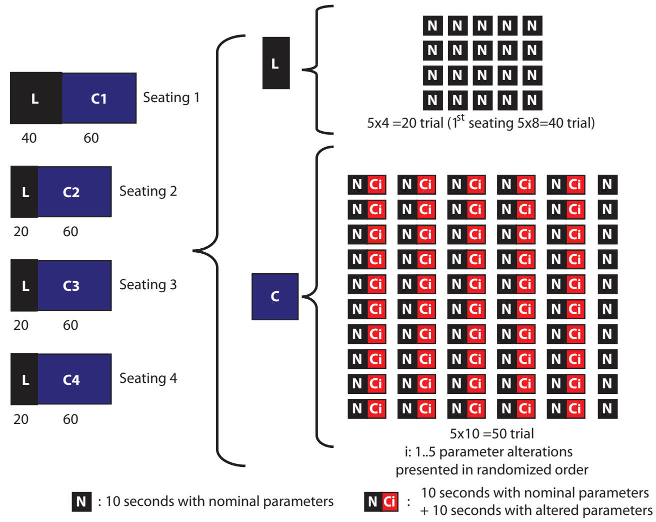

Figure 2: Experiment has four seatings, each with learning and catch sessions. In each seating, five different parameter sets are administered with catch trials. Each parameter set is randomly presented once in a catch trial block (five consecutive trials) and every block is repeated ten times.

2.3 Procedure

Participants sat in front of the monitor and held the haptic device with their dominant hand. Each trial was initiated with the mechanism and the two-mass system positioned at the neutral center of the work-space. The end-effector of the device was coupled with m_1 and users were provided with the occurring forces of the virtual second order system. The goal was to oscillate the virtual system at its natural frequency along the x-axis in a sinusoidal manner. Motion on the y-axis was constrained with a damped-cubic-stiffness force field. Participants were told that if the excitation was at the natural frequency of the virtual second-order system, the amplitude of oscillations of m_2 would be largest for constant amplitude excitation of the end-effector. Participants were also instructed to excite the system in using smooth natural movements of their hand.

A catch-trial experiment was conducted to test the effect of system parameters on rate of human adaptation. To do so, participants were overtrained with a nominal system of 1 Hz natural frequency and their adaptation to 1.4 Hz target natural frequency was tested, so that the experiments are compatible with the existing literature on human motor control of second order dynamic systems [6, 7]. Details of the experiment design are presented in Figure 2 and Table 1.

The experiment consisted of four seatings, each of which focused on a different set of parameter variations at the target frequency. Figure 3 presents the magnitude Bode plots of the position and impedance transfer functions for each seating. In particular, the gain value G of the transfer functions was changed in Seating 1, while the damping coefficient ζ was altered in Seating 2. In Seating 3, both the gain and damping parameters were changed simultaneously to check coupled effects. In Seating 4, the parameters were adjusted such that the peaks of the magnitude Bode plots were matched while the different damping ratios were set to investigate effect of different slopes on the magnitude plot.

At the start of each seating, participants were trained with an intense learning session (denoted with L in Figure 2) before catch trials were administered. On the first day, the learning session consisted of 40 trials of 10 seconds each with the nominal second order system of 1 Hz natural frequency, while on the later days of testing, 20 learning trials were completed, since it was sufficient to reach the same performance level achieved at the end of the first day. How-

Table 1: Experiment seatings, effect levels, nominal and target system parameters and the location of the related Bode plots are presented.

Seating	Task	Effect Levels	System Parameters	Related Figure
Low Freq. Nominal	-	-	$m_2 = 1kg$, $b = 2.4Ns/m$, $k = 40N/m$, $G = 0.272$ and $\omega_n = 1.066$	Low Freq. with Legend (0) in Figure 3
Seating 1	Gain Change	High Freq. Nominal	$m_2 = 0.8kg$, $b = 2.4Ns/m$, $k = 64N/m$, $G = 0.32$ and $\omega_n = 1.423$	Legend (1) in Figure 3
		G Lowest	$m_2 = 0.8kg$, $b = 2.4Ns/m$, $k = 64N/m$, $G = 0.128$ and $\omega_n = 1.423$	Legend (2) in Figure 3
		G Lower	$m_2 = 0.8kg$, $b = 2.4Ns/m$, $k = 64N/m$, $G = 0.224$ and $\omega_n = 1.423$	Legend (3) in Figure 3
		G Higher	$m_2 = 0.8kg$, $b = 2.4Ns/m$, $k = 64N/m$, $G = 0.416$ and $\omega_n = 1.423$	Legend (4) in Figure 3
		G Highest	$m_2 = 0.8kg$, $b = 2.4Ns/m$, $k = 64N/m$, $G = 0.512$ and $\omega_n = 1.423$	Legend (5) in Figure 3
Seating 2	Damping Change	High Freq. Nominal	$m_2 = 0.8kg$, $b = 2.4Ns/m$, $k = 64N/m$, $G = 0.32$ and $\omega_n = 1.423$	Legend (1) in Figure 3
		Damp Lower	$m_2 = 0.8kg$, $b = 2Ns/m$, $k = 64N/m$, $G = 0.32$ and $\omega_n = 1.423$	Legend (6) in Figure 3
		Damp Lowest	$m_2 = 0.8kg$, $b = 1.8Ns/m$, $k = 64N/m$, $G = 0.32$ and $\omega_n = 1.423$	Legend (7) in Figure 3
		Damp Higher	$m_2 = 0.8kg$, $b = 3.6Ns/m$, $k = 64N/m$, $G = 0.32$ and $\omega_n = 1.423$	Legend (8) in Figure 3
		Damp Highest	$m_2 = 0.8kg$, $b = 5.2Ns/m$, $k = 64N/m$, $G = 0.32$ and $\omega_n = 1.423$	Legend (9) in Figure 3
Seating 3	Gain and Damping Change	High Freq. Nominal	$m_2 = 0.8kg$, $b = 2.4Ns/m$, $k = 64N/m$, $G = 0.32$ and $\omega_n = 1.423$	Legend (1) in Figure 3
		Low Damp/High G	$m_2 = 0.8kg$, $b = 1.2Ns/m$, $k = 64N/m$, $G = 0.512$ and $\omega_n = 1.423$	Legend (10) in Figure 3
		High Damp/High G	$m_2 = 0.8kg$, $b = 5.1Ns/m$, $k = 64N/m$, $G = 0.512$ and $\omega_n = 1.423$	Legend (11) in Figure 3
		Low Damp/Low G	$m_2 = 0.8kg$, $b = 1.2Ns/m$, $k = 64N/m$, $G = 0.128$ and $\omega_n = 1.423$	Legend (12) in Figure 3
		High Damp/Low G	$m_2 = 0.8kg$, $b = 5.1Ns/m$, $k = 64N/m$, $G = 0.128$ and $\omega_n = 1.423$	Legend (13) in Figure 3
Seating 4	Common Peak Magnitude with Different Damping	High Freq. Nominal	$m_2 = 0.8kg$, $b = 2.4Ns/m$, $k = 64N/m$, $G = 0.32$ and $\omega_n = 1.423$	Legend (1) in Figure 3
		Lowest	$m_2 = 0.8kg$, $b = 1.2Ns/m$, $k = 64N/m$, $G = 0.16$ and $\omega_n = 1.423$	Legend (14) in Figure 3
		Lower	$m_2 = 0.8kg$, $b = 1.8Ns/m$, $k = 64N/m$, $G = 0.24$ and $\omega_n = 1.423$	Legend (15) in Figure 3
		Higher	$m_2 = 0.8kg$, $b = 3.0Ns/m$, $k = 64N/m$, $G = 0.40$ and $\omega_n = 1.423$	Legend (16) in Figure 3
		Highest	$m_2 = 0.8kg$, $b = 3.6Ns/m$, $k = 64N/m$, $G = 0.48$ and $\omega_n = 1.423$	Legend (17) in Figure 3

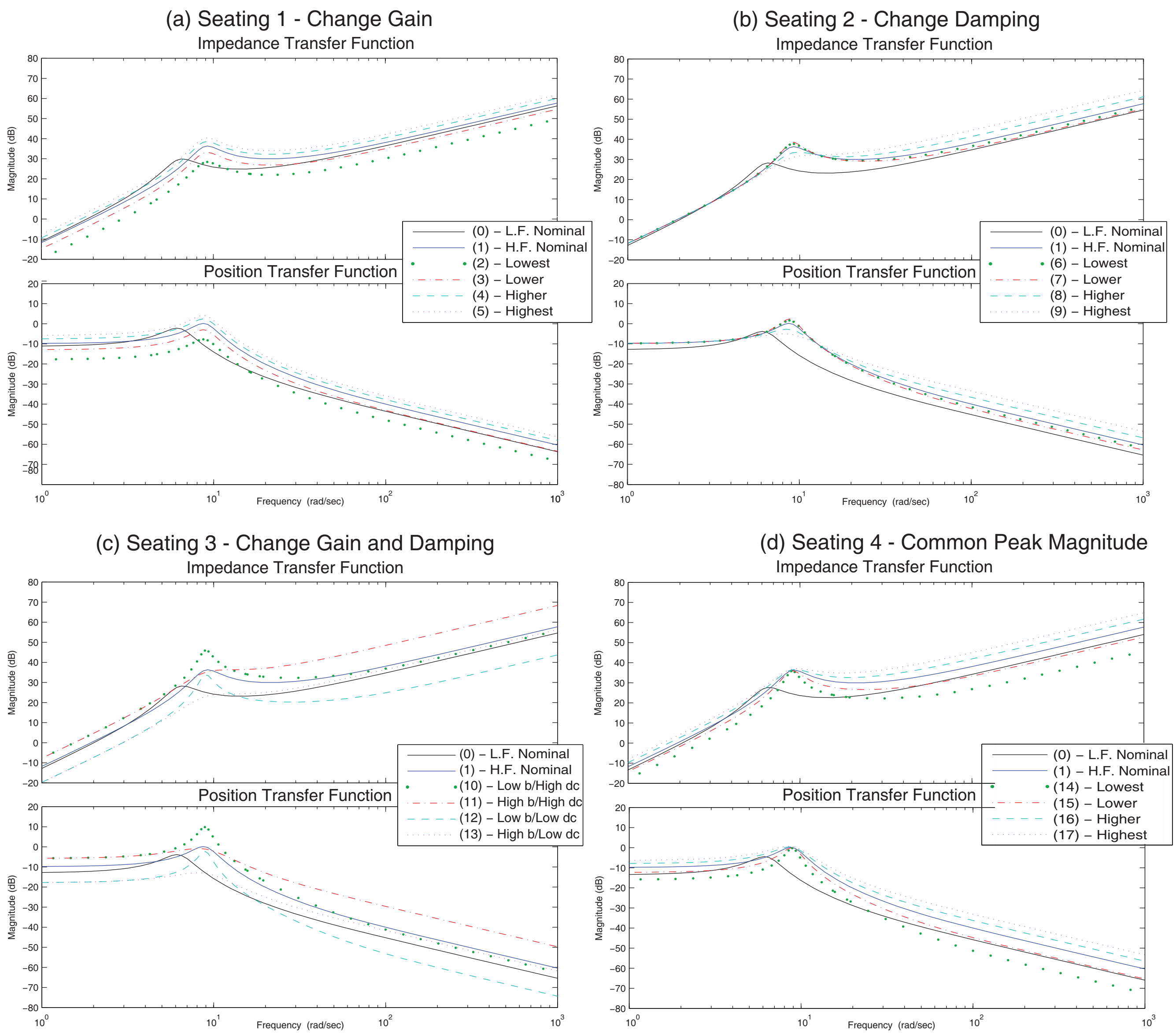

Figure 3: Magnitude Bode plots of the virtual systems used in the experiment. Position and impedance transfer functions of each system are plotted with the parameters given in Table 1.

ever, if the excitation frequencies for 8 out of last 10 trials were not within the 5-percent performance range, then the participants were asked to complete 10 more trials until the performance goal was met. All participants understood the task in the first 10 to 20 trials and were consistently exciting the nominal system at its natural frequency. Feedback about the performance of the participant was provided at every trial in learning session to correct any possible bias in the adaptation procedure. To provide feedback, frequency of excitation of the participant was compared with the natural frequency of the 1 Hz nominal system. A message indicating if oscillation frequency was greater than, lower than or within 5 percent of the system natural frequency was displayed so that the participant could increase, decrease or maintain their input frequency.

At each seating, following the completion of the learning session L, participants attended catch trial sessions (shown as $C1$ to $C4$ in Figure 2). There existed 5 different parameter sets in each seating, which were randomly presented to the user within a block (five consecutive catch trials) of the experiment. These parameter sets are indicated by the five frequency response plots in each panel of Figure 3. Repetition of this block for ten times in every catch session resulted in 50 trial sets. Between every block, a learning set trial was administered to the user with feedback provided, in order to help wash out the effects of catch trials. Each catch trial lasted 20 seconds; for the first 10 seconds the participants excited the nominal system at 1 Hz. After this, the virtual system parameters were changed to one of the randomly selected parameter sets of the appropriate seating with a natural frequency of 1.4 Hz. The participants adapted to the new dynamics at 1.4 Hz and excited this new system within the next 10 seconds of the catch trial.

Table 1 lists each seating, the effect levels, the system parameters used to implement the virtual systems and the location of the related magnitude Bode plots of position and impedance transfer functions (Eqns. (3) and (4), respectively). Each of the four seatings focused on the effects of different system parameter variations; however, one parameter set was kept the same throughout all catch sessions ('High Freq. Nominal' values in Table 1) in order allow for cross comparisons.

2.4 Data Analysis

Displacement and velocity data of end effector (m_1) and m_2 were collected at 500 Hz during every trial. For 20 seconds of trials, a total of 10000 data points are acquired for each parameter set for every catch session. The hand excitation data was processed in Matlab using time-frequency scripts[1]. The preprocessed data was down sampled to 50 Hz and then passed through a 129-point Hamming window. The spectrogram (time-frequency trajectories) profiles were obtained and the frequencies with the maximum power content at each instant of time were extracted. A plot of frequency as a function of the duration of a catch trial is given in Figure 4. One can observe the variation of hand excitation frequency while adapting from the 1 Hz nominal system to the 1.4 Hz target system.

The goal of each catch session is to evaluate the effect of particular parameter sets on adaptation of hand excitation frequency between nominal and target system, primarily focusing on rate of adaptation and steady state error. Since each set of parameters was provided to participants for ten times in a catch session, average value of the recorded data for each set was taken after calculating frequencies with maximum power content at every time instant. Subsequently, an exponential fit with three parameters (L_0, L_∞ and τ) was performed according to the formula: $F = L_0 - (L_0 - L_\infty)\, e^{-\tau t}$. In this equation, L_0 represents the starting frequency, L_∞ is the steady state value after adaptation, while τ (the time constant of the exponential function) models the rate of adaptation. Since the change in parameters were administered at the 10th second of a catch trial, the exponential curves were fitted

[1] Available at http://tftb.nongnu.org/ for download

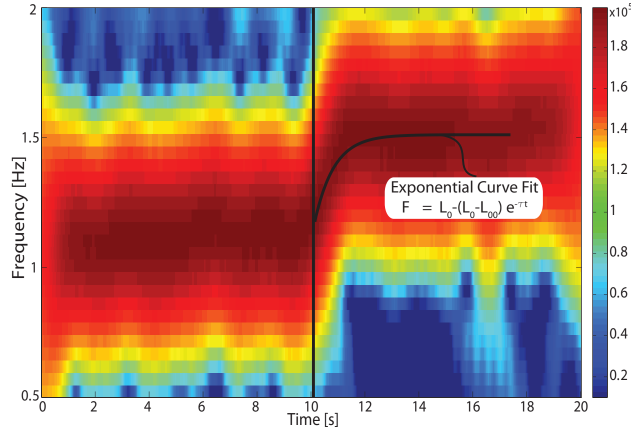

Figure 4: Frequency spectrum as a function of time for a sample catch trial. Exponential fit for the trial is also presented.

on the data starting from this instant. To determine the L_0 parameter, the average frequency of excitation between the 8th and 10th seconds of the catch trial were used.

One factor repeated measure ANOVAs (Analysis of Variance) were used to determine significant differences (alpha=0.05) among the five systems in each seating conditions. Multiple pair wise comparisons were performed by using Bonferroni Confidence interval adjustments.

3 Results and Discussion

For ten seconds in every trial, the parameter set for low frequency was used which was overtrained by the participant. After these ten seconds, a catch occurred where the system parameters were altered to present a system with higher frequency response. Data acquired from all sessions were processed as detailed in Section 2.4, and performance measures were analyzed in order to examine the human response to system dynamics alteration; the rate of adaptation is (τ) and the steady state excitation frequency for the catch system (L_∞). A third variable L_0 measures the steady state excitation frequency for the overtrained 1 Hz nominal system dynamics. For each of the catch trials, L_0 values were observed to be within the JND value of 1 Hz (within $\pm 4\%$ of 1 Hz).

3.1 Seating 1 – Varying Gain

In Seating 1, the effects of changing gain G on human adaptation was studied. Two target systems with higher and two target systems with lower gain values than the high frequency nominal system were tested. The parameters for the four target systems are summarized in Table 1. The Bode plots of target systems are given in Figure 3 (a).

It was hypothesized that increasing the gain will decrease steady state error while increasing the time of convergence. Results indicate that the change of gain G has no statistically significant effect on the steady state frequency values, L_∞ $[F(4,24) = 0.9; p = 0.47]$. However, the rates of adaptation are significantly affected by altered gain values.

Figure 5 presents the rate of adaptation results for Seating 1. In particular, box plots of τ values are shown for each level of gain parameter and statistically significant interactions with $p < 0.05$ are marked. There is a significant difference in the adaptation rates for 'lowest' gain level and all other gain levels. There are also significant differences in the adaptation rates between 'lower' and 'highest' gain levels. Systems with intermediate gain values were not significantly different from each other in terms of adaptation rates; however, there exists an overall trend for the mean values indicating a monotonic decrease of adaptation rates as the gain is increased.

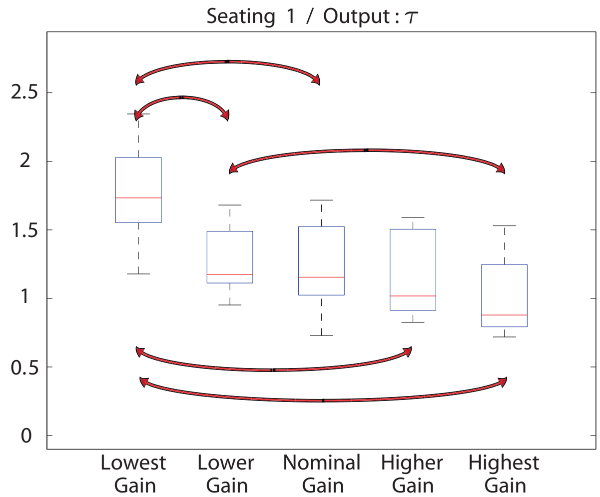

Figure 5: Box plots for Seating 1 for varying gain G values. Statistically significant pairs with $p < 0.05$ are marked.

The fact that the change in gain does not effect L_∞ values is in agreement with the recent findings in the literature [6] which state that humans can robustly identify the natural frequency of a second order system and excite it at this natural frequency even when the magnitude cues are changed. On the other hand, the adaptation rate is significantly affected in such a way that the rate of adaptation decreases as the gain is increased. Since, when the gain is increased, the required effort to complete the task increases, the decrease in adaptation rate can be attributed to the inherent trade-off between task performance and effort in human motor control.

3.2 Seating 2 – Varying Damping

The second seating studied effects of the changing the damping ratio b of the system. Two target systems with higher and two target systems with lower damping ratios than the high frequency nominal system were tested. The parameters for the four target systems are summarized in Table 1. The Bode plots of target systems are given in Figure 3 (b).

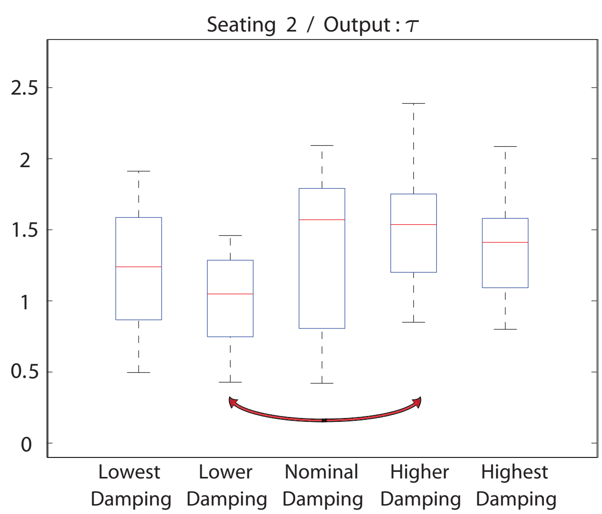

Figure 6: Box plots for Seating 2 for varying damping ζ values. Statistically significant pairs with $p < 0.05$ are marked.

It was hypothesized that increasing the damping will have a stabilizing effect on human motor control, while perception of the natural frequency will be diminished. Results indicate that all of steady state frequency values L_∞ except for the 'highest' damping level are within the JND at 1.4 Hz. There exists a statistically significant difference with $p < 0.05$ in the L_∞ value for 'highest' damping set and all other sets. In particular, participants overshoot the target frequency with an average error of 0.16 Hz with the 'highest' damping level.

Figure 6 depicts the rate of adaptation results for Seating 2. In particular, box plots of τ values are shown for each level of damping parameter and statistically significant interactions with $p < 0.05$ are marked. There exists a statistically significant difference between adaptation rates with 'lower' and 'higher' damping levels, indicating faster adaptation with the increased damping level. The mean values of adaptation rates exhibit a monotonically increasing trend as the damping is increased from 'lower' to 'higher' level. The adaptation rates seem to saturate out of these levels, that is, the monotonic trend flattens at extremes. In particular, the means of 'lowest' and 'lower' levels and the means of 'highest' and 'high' levels stay close to each other.

The steady state frequency overshoot with the 'highest' damping level may be attributed to decreased human perception due to the diminished peak of the magnitude Bode transfer function. The increase of the rate of adaptation as the damping is increased within a certain range may be attributed to the stabilizing effects of damping beneficially affecting the human excitation.

3.3 Seating 3 – Varying Gain & Damping

Seating 3 investigated aggregated effects of simultaneous changes in damping and the gain parameters of the system. In addition to the high frequency nominal parameter set, the test conditions included lower damping, higher gain (low b / high G); higher damping, higher gain (high b / high G); lower damping, lower gain (low b / low G) and higher damping, lower gain (high b / low G) systems. The parameters for the four target systems are summarized in Table 1. The Bode plots of target systems are given in Figure 3 (c).

Figure 7 depicts steady state frequency and the rate of adaptation results for Seating 3. In particular, box plots of L_∞ and τ values are shown for each level of damping parameter and statistically significant interactions with $p < 0.05$ are marked. The experiment results indicate that the steady state frequency for the nominal parameter set and the parameter sets with 'low' damping values fall within JND at 1.4 Hz. However, the parameter sets with 'high' damping values overshoot the steady state frequency regardless of the value of the gain parameters. The difference among the 'low' and 'high' damping sets are statistically significant. The rate of adaptation results indicate a statistically significant difference between opposite pairs of parameters, with 'low damping-high gain' parameter set exhibiting a lower rate of adaptation than 'high damping-low gain' set. There also exists a trend among 'low' gain and 'high' gain parameter sets, indicating lower adaptation rates for high gain systems when compared to low gain ones.

The steady state frequency results are consistent with Seating 2, and the overshoot may be attributed to the effect of damping on the magnitude transfer function and impact on human perception. The adaptation rate results are consistent with Seating 1, confirming that as the gain (required effort for the task) increases, the task performance decreases.

3.4 Seating 4 – Common Peak Magnitude

In Seating 4, the parameters were adjusted such that the peaks of the magnitude Bode plots were matched at the natural frequency of the target systems, while different damping ratios were set to test effect of different slopes on the magnitude plots. Two target systems with 'higher' and two target systems with 'lower' damping (slope) than the high frequency nominal system were tested. The parameters for the four target systems are summarized in Table 1. The Bode plots of target systems are given in Figure 3 (d).

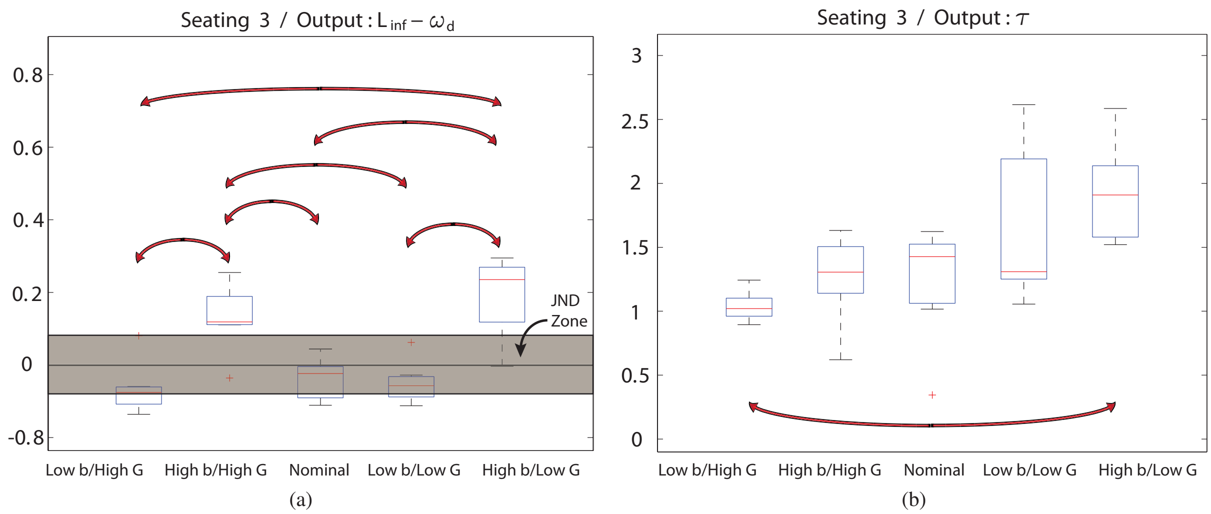

Figure 7: Box plots for Seating 3 for varying gain G and damping ζ parameters simultaneously. Statistically significant pairs with $p < 0.05$ are marked.

Results indicate that all of steady state frequency values L_∞ are within the JND at 1.4 Hz. Similarly, there exists no statistically significant difference in the τ values among the parameter sets $[F(4,24) = 0.19; p = 0.94]$.

These results are consistent with the previous results, providing evidence that the gain of the Bode magnitude plots is an important factor effecting the rate of adaptation. The results also indicate that when the gains of the systems are normalized around the operating point (natural frequency of the target system), the effect of damping parameter is insignificant for the tested range of damping values.

4 Conclusions

We explored the effects of dynamic response and parameters of a second order dynamic system on human motor adaptation while performing a rhythmic dynamic task. The results of the experiment with four seatings demonstrate that parameters of a dynamic system have significant effects especially on the rate of human motor adaptation. Results provide evidence that the rate of adaptation is strongly related to the required effort to complete the task and that the rate of adaptation decreases as the effort to complete the task is increased. Along these lines, the results also indicate that scaling of haptic feedback significantly affects the rate of adaptation.

The results are important in that they suggest a trade-off on use of haptic feedback. On one hand, haptic feedback may positively affect the perception of the task dynamics beneficially affecting the task performance, while on the other hand too much haptic feedback may have detrimental effects due to increase in the required effort to complete the task.

In order to distinctly analyze the effects of haptic and visual feedback, additional experiments using equivalent systems are being conducted. In particular, using systems with identical position transfer functions, we can render different forces to the user for the same visual output, while utilizing equivalent systems with identical impedance transfer function, the same level of forces can be fed back to the user for different visual outputs. Initial results of these experiments are in good agreement with the results of this paper. Determination of the optimal level of haptic feedback for the second order virtual resonance task is left as future work.

Acknowledgements

This work was supported in part by TUBITAK 107M604 grant. Portions of this work were supported by the National Science Foundation under Grant No: IIS-0448341 and Grant No: IIS-0812569. The authors thank Hakan Kapson for his help in conducting the preliminary experiments.

References

[1] N. Bhushan and R. Shadmehr. Computational nature of human adaptive control during learning of reaching movements in force fields. *Biological Cybernetics*, 81(1):39, 1999.

[2] J. B. Dingwell, C. D. Mah, and F. A. Mussa-Ivaldi. Manipulating Objects With Internal Degrees of Freedom: Evidence for Model-Based Control. *J Neurophysiol*, 88(1):222–235, 2002.

[3] J. B. Dingwell, C. D. Mah, and F. A. Mussa-Ivaldi. Experimentally Confirmed Mathematical Model for Human Control of a Non-Rigid Object. *Journal of Neurophysiology*, 91(3):1158–1170, 2004.

[4] F. C. Huang, R. B. Gillespie, and A. D. Kuo. Visual and haptic feedback contribute to tuning and online control during object manipulation. *Journal of Motor Behavior*, 39(3):179 – 193, 2007.

[5] J. Huegel and M. O'Malley. Visual versus haptic progressive guidance for training in a virtual dynamic task. In *EuroHaptics conference and Symposium on Haptic Interfaces for Virtual Environment and Teleoperator Systems. World Haptics. Third Joint*, pages 399–400, 2009.

[6] A. Israr, H. Kapson, V. Patoglu, and M. O'Malley. Effects of magnitude and phase cues on human motor adaptation. In *EuroHaptics conference, 2009 and Symposium on Haptic Interfaces for Virtual Environment and Teleoperator Systems. World Haptics 2009. Third Joint*, pages 344 –349, 2009.

[7] A. Israr, Y. Li, V. Patoglu, and M. K. O'Malley. Passive and active discrimination of natural frequency of virtual dynamic systems. *IEEE Transactions on Haptics*, 2:40–51, 2009.

[8] J. W. Krakauer, M.-F. Ghilardi, and C. Ghez. Independent learning of internal models for kinematic and dynamic control of reaching. *Nature Neuroscience*, 2(11):1026, 1999.

[9] Y. Li, J. C. Huegel, V. Patoglu, and M. K. O'Malley. Progressive shared control for training in virtual environments. *World Haptics Conference*, 0:332–337, 2009.

[10] J. Patton and F. Mussa-Ivaldi. Robot-assisted adaptive training: custom force fields for teaching movement patterns. *Biomedical Engineering, IEEE Transactions on*, 51(4):636 –646, 2004.

[11] R. Shadmehr and O. A. Mussa-ivaldi. Adaptive representation of dynamics during learning of a motor task. *Journal of Neuroscience*, 14:3208–3224, 1994.

[12] D. Sternad, M. Duarte, H. Katsumata, and S. Schaal. Bouncing a ball: Tuning into dynamic stability. *Journal of Experimental Psychology: Human Perception and Performance*, 27(5):1163 – 1184, 2001.

[13] M. Svinin, I. Goncharenko, Z.-W. Luo, and S. Hosoe. Reaching movements in dynamic environments: How do we move flexible objects? *Robotics, IEEE Transactions on*, 22(4):724 –739, 2006.